ORIGINAL ARTICLE

lajss.org© Latin American Journal of Solids and Structures

www.lajss.org

Validation of Finite Element Models for the Earthquake Simulator of Steel Storage Racks Using Full-Scale Shaking Table Tests

Fuat Yılmaz[a]* , Fatih Alemdar[a]

[a] Yıldız Technical University, Faculty of Civil Engineering, Department of Civil Engineering, Structural Division, Davutpaşa Campus, 34210 Esenler, Istanbul, Turkey. Email: fuadeng5@gmail.com, falemdar@yildiz.edu.tr

* Corresponding author

https://doi.org/10.1590/1679-7825/e9003

Abstract

This study investigates the down-aisle seismic performance of a full-scale 3D cold-formed steel rack system using shaking table tests. The rack system was tested using scaled Northridge earthquake records, and the dynamic responses were evaluated during the test. The results demonstrated that the rack response remained essentially elastic up to approximately 50% of the Northridge intensity, beyond which pronounced inelastic behavior, approximately 50% stiffness degradation, and permanent drifts were observed. The experimental results were validated using an FE analysis, with substantial agreement in the elastic-to-mildly inelastic range, with similarity ratios of approximately 80%. However, differences were observed in the response values at the higher excitation intensities due to the high pallet sliding and connection slip during the test, which could not be accurately reflected in the FE model. It was observed that pallet sliding and connection friction, rather than member strength alone, governed the response under strong shaking and should be explicitly considered in advanced numerical models and in the seismic assessment of steel racks.

Keywords

Shaking table test, Finite element analysis, Storage rack systems, Down-aisle direction, Seismic analysis.

Graphical Abstract

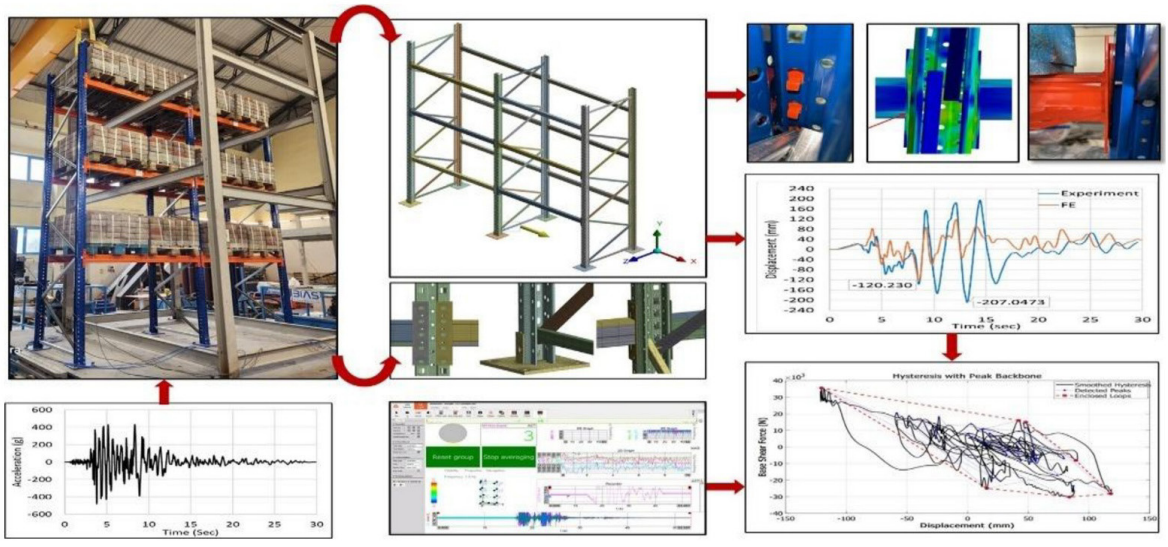

Received February 07, 2026. In revised form April 06, 2026. Accepted April 24, 2026. Available online April 28, 2026.
https://doi.org/10.1590/1679-7825/e9003

1 INTRODUCTION

Steel storage racking systems are structures manufactured from cold-formed steel and hold a prominent position in the industrial market owing to their high storage efficiency in small spaces relative to their light weight. Rapid industrial development has created a significant demand for these systems, and their use has expanded considerably recently because of the growth in the transportation and storage of goods in large factories and logistics firms. Although the cost of storage racks is relatively reasonable because they are manufactured from cold-formed components, ensuring their safety is crucial, particularly when they are subjected to dynamic loads such as earthquakes. Any partial damage to a rack component can cause partial or complete collapse of the racking system, resulting in significant economic or human losses in the areas where these systems are located.

Standard storage racking systems are classified into two types based on their structural configuration: braced and unbraced. In the industrial market, unbraced rack systems are preferred over braced systems in the aisle direction to facilitate product placement, loading, and unloading processes. Generally, the braces in the transverse (cross-aisle) direction control the racks' resistance to lateral forces, whereas in the longitudinal aisle (down-aisle) direction, lateral loads are resisted by the moment frames, which are significantly affected by the behavior of the beam-upright connections in that direction.

Storage racking systems are often designed to facilitate efficient loading and unloading operations in warehouses. Moment-resisting frames are arranged along the longitudinal aisle, and vertical posts are supported by transverse braces perpendicular to the aisle direction, thereby increasing the rack stability. The structural performance of these systems cannot be accurately determined using the traditional analytical methods used for other structures because of their complex behavior. This complexity arises from the manner in which the vertical uprights are fixed to the ground using bolted baseplates without constraints at the upper edges, as well as the complicated behavior resulting from friction between the connections of the rack members. In designing storage racking systems, it is difficult to find a balance between safety, regulations, and economic feasibility, as is often the case in traditional structural-design approaches. Consequently, the design processes for storage racks are frequently imprecise owing to an incomplete understanding of their complex behavior and responses to dynamic loads, such as seismic loads.

In their shaking table tests on the effect of viscous damping, base plate property, and sliding of the loading pallet on the collapse mechanism and energy dissipation capacity of rack systems, Jacobsen and Tremblay (2017) showed that linear models with equivalent viscous damping and secant stiffness cannot reproduce energy dissipation as accurately as nonlinear models, but they did not propose a generalized numerical FE model or study a wider range of rack geometries and connection details, limiting the broader applicability of their results.

Maguire et al. (2020) evaluated the cross-aisle seismic performance of racks with different baseplate fixities using single-axis shaking table tests, showing that all baseplates met design-level demands, rigid baseplates failed at 150% intensity, and ductile baseplates survived up to 230%; however, the study considered only one rack geometry and baseplate arrangement, limiting generalization to other configurations.

Firouzianhaji et al. (2021) proved that the response acceleration, displacements, and base shear force of the storage rack system increased as the seismic input increased up to full scale. The test results demonstrated an increase in the damping ratio and energy dissipation capacity owing to the sliding of the pallet, particularly in the large response behavior. Their study did not develop or validate a detailed finite element model to generalize these findings to other rack configurations and loading conditions.

Shaheen and Rasmussen (2019) evaluated the load distribution, stiffness loss, and failure types of rack systems in the cross-aisle direction through full-scale shaking table tests on various configurations of rack systems. Their study demonstrated that ductile failure mechanisms and a higher uniform load distribution were observed when the rack system was provided with horizontal braces at the upper connections in the cross-aisle direction. The relative stiffness, load transfer property, hardening property, and plastic moment of the rack connections of storage rack systems were investigated through static and cycling loading tests (Gilbert and Rasmussen, 2010; Aguirre,2005).

Kanyilmaz et al. (2016) analyzed the behavior of the storage rack system by assessing pushover tests on fully loaded steel storage rack structures with no braces in the down-aisle direction. The results showed that in the first stage of loading, plastic hinge formation occurred in the uprights associated with concentrated stresses at the joints located on the first floor, leading to brittle failure and inadequate stiffness of the baseplate connections. However, their study only examined racks under monotonic pushover loading; therefore, the results on ductility and failure modes cannot be generalized to other rack configurations or real earthquake actions.

Castiglioni et al. (2003) studied the influence of the diagonal bracing position on the seismic behaviour of the two aisles of rack systems designed according to Eurocode 8 through full-scale shaking table tests. They concluded that eccentric bracing designs cause significant torsional behavior and that the position of the diagonal bracing plays an important role in the seismic response of rack systems.

In their study, Filiatrault and Wanitkorkul (2004) performed uniaxial shaking table experiments on five back-to-back rack systems to evaluate their seismic responses in both cross- and down-aisle directions. Their results concluded that the rack system exhibited adequate response in the down-aisle direction in terms of ductility, flexibility, and energy dissipation capacity.

In their comparative evaluation between the modal response spectrum and nonlinear time-history approaches, Bernuzzi and Simoncelli (2017) showed that slenderness, bracing, and live-load participation markedly influenced seismic demands; however, they considered only a limited set of code-designed pallet rack prototypes and did not validate their advanced design strategies with full-scale experiments, limiting direct application to other rack systems.

Saravanan et al. (2014) studied the dynamic response of a three-dimensional, two-story, single-bay pallet rack with hooked connectors through shake-table experiments. Complementary finite-element modeling: This was carried out with connector stiffness values obtained by Prabha et al. (2010), who managed to recreate the experimentally obtained dynamic characteristics, thus proving that there is a correlating factor between the numerical simulations and the physical test results.

In their investigation of the seismic performance of pallet-type steel storage racks that store palletized goods on slightly sloped shelves to reduce the risk of merchandise falling off, Sideris et al. (2010) conducted shake table and pull tests to study the dynamic response of these rack systems under earthquake loading conditions. The effectiveness of the inclined shelving concept was highlighted by the shaking table results, which indicated that a modest shelving inclination of 3.5° successfully eliminated seismic-induced pallet falling for the tested ground motion.

Many prior studies have evaluated the stiffness, elastic, and plastic responses of storage racks using nonlinear pushover analyses under earthquake excitation. Nuñez et al. (2020) demonstrated that the overall stiffness of stiffer systems was increased, resulting in a higher base shear, but the seismic performance was still acceptable. In his investigation, Carr A. (2016) showed that because of the general rack structural flexibility, the lower stiffening in the rack results in large amounts of lateral displacement and large column moments.

As revealed in the studies conducted by Petrone et al. (2016) and Gwanghee Heo et al. (2023), the seismic response of rack systems is influenced by the thickness of the baseplate connections and fixity conditions; sufficiently low baseplate resistance can initiate collapse owing to the large externally imposed displacement. Çelik et al. (2022) investigated low-rise single-module pallet racks in the down-aisle direction using full-scale pushover tests and validated 3D shell FE models to study how different base plate types and bracing layouts affect stiffness, torsional behavior, and energy dissipation; however, their study was limited to static pushover analysis and did not examine dynamic seismic response under real earthquake loading.

Drei et al. (2014) demonstrated that strategic external bracing and precision-engineered connections significantly enhance the lateral stiffness and global system performance under lateral loads, primarily by enabling controlled energy dissipation. Petrovčič and Kilar (2012) numerically examined a high-rack steel structure and showed that horizontal and vertical mass asymmetries can significantly amplify and unevenly distribute seismic demands; however, their study was limited to a single rack model and lacked experimental validation, restricting the generality of their conclusions.

Advancements in experimental testing have provided valuable insights into the performance of storage rack systems; however, the high costs and significant time requirements associated with these tests remain substantial challenges. Consequently, validated numerical modeling approaches have emerged as efficient and reliable tools for optimizing rack system designs while ensuring structural integrity, as demonstrated in recent studies (Bové et al., 2021; Chen et al., 2019; Vujanac et al., 2020; Bonaventura et al., 2021).

There are no globally recognized design codes for storage rack systems, combined with the partial nature of seismic design evidence found to date, which highlights an enormous gap in the protection of these systems that are both economically required and highly functional. Even when such standards are available, they are often considered as recommendations rather than building rules, which further emphasizes the necessity of in-depth, full-scale experimental research to clarify the global seismic response of rack systems.

Despite extensive research on steel storage rack systems, significant gaps remain that have not been thoroughly investigated because of their structural complexity. Most existing studies have focused on the cross-aisle direction, which is typically braced for stability. In contrast, the down-aisle direction often lacks bracing owing to operational and accessibility requirements, resulting in reduced lateral stiffness and strength. This leaves a significant gap in the understanding of the seismic performance and failure mechanisms of rack systems in the down-aisle direction, especially during large seismic intensities, so that the loading pallet sliding on the rack beams or the friction of the connections causes asymmetric loading and recentering problems during the shaking time, which may lead to an increase in lateral displacement, stiffness loss, and then partial or overall collapse of these structures. This study addresses this gap by focusing on the comparatively scarcely studied seismic dynamics of storage racks, specifically by focusing on asymmetric loading scenarios caused by pallet movement in the down-aisle direction during the shaking test. The research results provide new empirical data points that can be employed to develop more effective seismic threshold designs and help understand how the movement of loading pallets and the friction between the connections and rack components affect the seismic response, damping, and stiffness loss of rack structures during seismic loading.

Many numerical studies have neglected the presence of perforations and tabs in the assembly of rack systems in their analyses. However, these features can significantly decrease the critical buckling load of the uprights and alter the local deformation patterns, leading to inaccurate predictions of the system behavior. This study addresses this gap by integrating highly detailed finite element models using ANSYS Workbench to respond to all salient geometrical, material, and connection behaviors, such as perforations and tabs. This study provides a realistic simulation of rack system behavior. The findings of the finite element analysis were experimentally verified using shake table tests under different scale excitations of the Northridge earthquake records. This study also covers the gaps in the effect of the loading pallet movement on the response displacement of rack systems in the case of seismic events. The results of this study provide excellent insights into the effects of element dimensions, system geometry, and mass eccentricity on the seismic performance of these systems.

2 MATERIALS AND METHODS

2.1. Geometric and mechanical properties of the storage racks

In general, storage rack structures are non-structural lightweight structures that can be categorized into different types according to their form and structure. These systems can withstand heavy loads adequately compared with their light weights. In this study, a three-level standard pallet rack system with two spaces (Figure 2) was considered and designed according to the CFS profiles (Figure 1) used in the Turkish market to evaluate the actual dynamic response and study the effect of pallet sliding on the dynamic characteristics of such structures through real experimental tests under seismic events. The dimensions of the considered rack system were selected according to the user's requirements, and the width in the down-aisle direction of the rack was determined such that two Euro standard loading pallets with dimensions of 800 × 1200 × 145 mm could be placed on the beams of the rack, as shown in Figure 5.

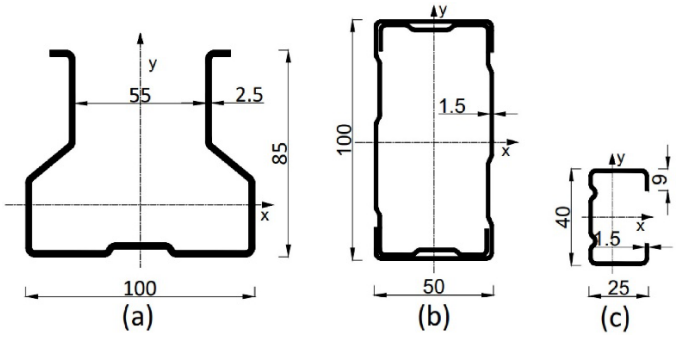

Figure 1 Section details (dimensions in mm): (a) upright, (b) beam, and(c) diagonal brace section.

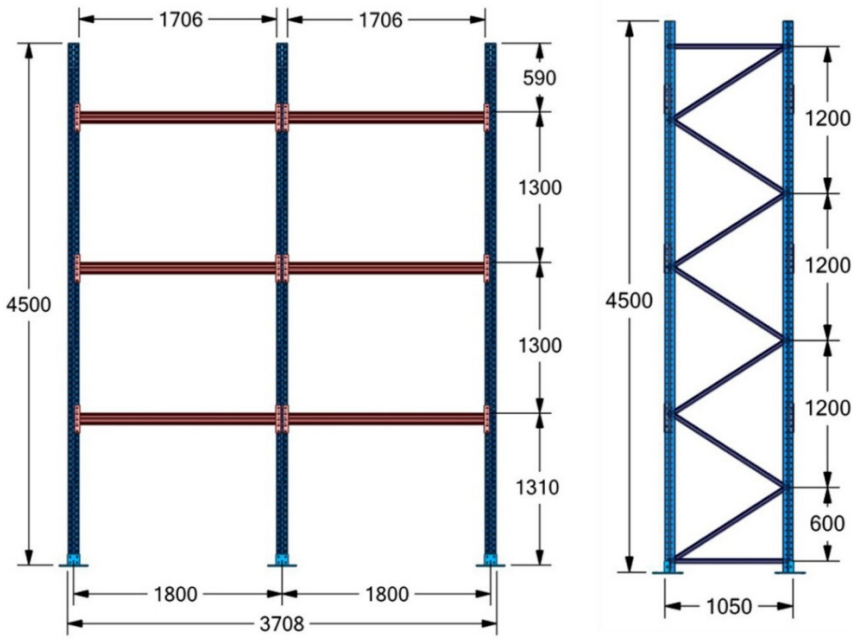

Figure 2 Dimensions of the storage rack system (units: mm).

Cold-formed steel components, including uprights, beams, diagonal braces, and connections, were used in the rack system (Figure 1). A 100x85x2.5 mm Omega section was used in the uprights, a 100x50x1.5 mm front-to-front C section was used in the beams, and the diagonals were designed using a 40x25x1.5 mm C section. The system was fixed using four M10x25(8.8) bolts to the shaking table platform using a 250x250x10 mm base plate connection. M10(8.8) bolts were used to assemble the column-bracing connection in a direction perpendicular to the aisle. The connection between the uprights and beams was established using safety pins in the beam connector to prevent any expected separation between them during the test process. The geometric and mechanical properties of the rack components are listed in Table 1.

Table 1 Mechanical properties of CFS sections used in the rack system.

Section	B(mm)	H(mm)	t (mm)	Ag (cm2)	Ixx(cm4)	Iyy(cm4)
Upright	100	85	2.5	7.329	136.229	255.047
Travers	50	100	1.5	6.360	263.393	64.987
Diagonals	25	40	1.5	1.512	9.782	2.727

2.2. Material properties

Storage rack systems are generally produced using cold-formed steel members. Two types of materials were considered for the rack system. One for the uprights and the other for the traverses and diagonals. In this study, to evaluate the mechanical characteristics and nonlinearity behavior of the materials used in the rack structure considered for finite element numerical validation, tensile coupon tests were conducted on 6 plate samples with thicknesses of 2.5 and 1.5 mm. The results of these tests were measured, and the average values (Table 2) were used to characterize the actual elastic and plastic behaviors of the materials. The resulting stress-strain relationship of the considered materials with an elasticity modulus of 200 GPa and Poisson's ratio of 0.3 is shown in Figures 3 and 4.

Table 2 Tensile test results of coupons (CFS).

	Thickness =2.5 mm			Thickness = 1.5 mm		
	Fy (Mpa)	Fu (Mpa)	Elongation (%)	Fy (Mpa)	Fu (Mpa)	Elongation (%)
Coupon 1	423	538	20.79	285	404	26.39
Coupon 2	425	535	20.04	274	399	32.31
Coupon 3	422	535	27.21	275	401	27.10
Average	423.00	536.00	22.68	**278**	**401**	**28.54**

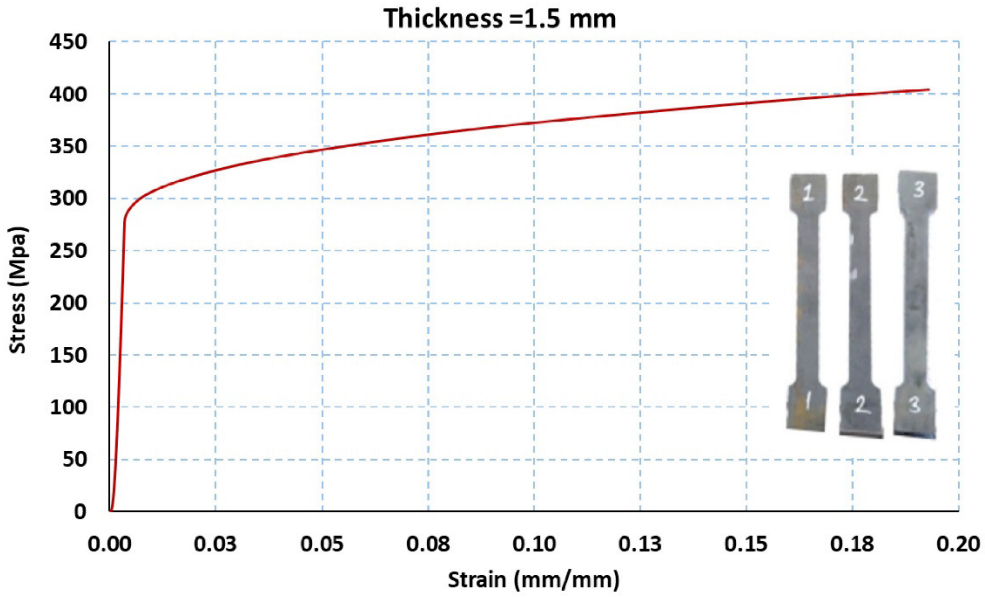

Figure 3 Stress-strain relationship for the cold-formed steel material used in the traverses and diagonals.

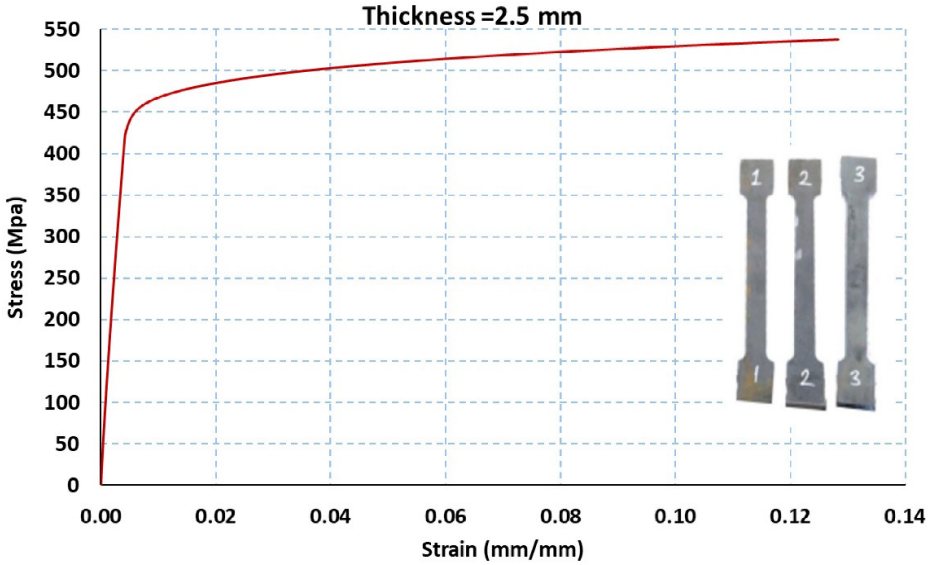

Figure 4 Stress-strain relationship for the cold-formed steel material used in the upright section.

3 EXPERIMENTAL SHAKING TABLE TEST

3.1. Shaking Table Test

This study analyzed the dynamic behavior of a storage rack system under seismic loading conditions. For this purpose, a full-scale rack system was constructed and tested using a shaking table platform located at the Damping Support Test Center of the Civil Engineering Department at Yıldız Technical University. The dimensions of the shaking table platform used were 4 m × 4 m, with freedom of movement in two perpendicular directions, a vertical load capacity of 500 kN, and a horizontal load capacity of 400 kN. The shaking table platform can apply an acceleration of 4.48 g and can reach a speed of 1 m/s with a simple frequency of 1000 Hz, capable of displacing up to ±0.5 m. Uniaxial accelerometers with a simple frequency of 1000 Hz and a capacity of ± 50 g were used in the test. The test was conducted by installing the pallet rack on the shake table, as shown in Figure 5.

Figure 5 Shaking table test setup of cold-formed rack system.

The rack structure was loaded with 12 wooden pallets weighing 1.040 tons to simulate the cargo loaded on the rack system. A load of 4.16 tons was applied to each level, such that the total vertical load on the system was 12.48 tons. The pallets were not fixed to the beams to represent the actual loading of the pallet rack system and to evaluate the expected fall damage that may occur during the test, as shown in Figure 6.

Figure 6 Details of the rack components.

Different scales, ranging from 10% to 100% of the Northridge earthquake (Figure 7), were used as input excitations in the experimental tests to evaluate the dynamic behavior, stiffness degradation, and linear or nonlinear behavior of the storage rack system. During the experimental test, the collapse situation, buckling, response displacement, and acceleration of the rack system were evaluated. Furthermore, the effects of pallet sliding and connection friction on the permanent displacement, damping mechanism, and energy dissipation capacity of the system were assessed.

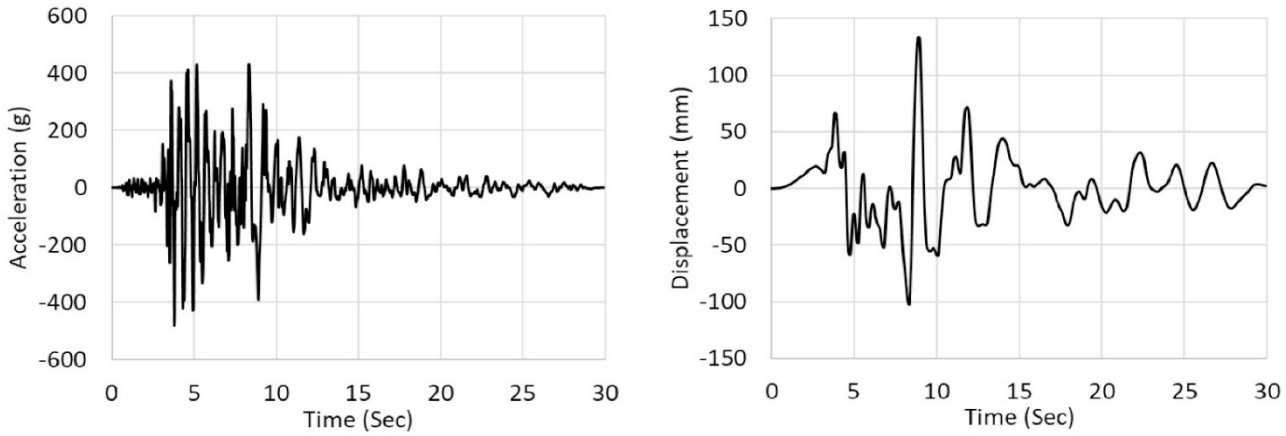

Figure 7 Time history of the Northridge earthquake records.

After each shaking table test, the system was excited with white noise with a frequency range of 0.3–20 HZ to determine the changes in the damping ratio and delay rate of the dynamic response. The results obtained for the damping ratio of the rack system were used as input variables in the finite element analysis validation to capture the actual behavior of the rack system under the same seismic intensities.

3.1. Experimental Results

During the shake table test, four displacement sensors were used at each pallet rack level. Three of them were mounted at each level on the uprights to measure the displacement response in the down-aisle direction, and another displacement sensor was mounted on the top of the other upright of the rack system to measure the displacement following torsion and subsequently the torsional capacity of the system (Figure 8).

Figure 8 Accelerometer sensor and LVDT placement on the rack structure.

According to the experimental test results under the full scale of the Northridge earthquake, small tears in the holes of the uprights, plastic deformation, and local paint cracks were observed at the beam-upright connections, indicating concentrated damage at these connections. However, the main components of the rack structure, such as the uprights and beams, were not affected by any noticeable general torsional or fracture failure. A small, slight deformation and crushing in the paint and slight ovalization near the connection regions were observed, as shown in Figure 9. This is evidence of local bearing yielding rather than bolt shear failure in these regions, but not overall buckling or fracture of the entire plate. This type of damage can reduce the stiffness of the rack structure by concentrating more load on fewer brace elements. No noticeable plate yielding or uplift was observed at the baseplate connection during the test. This indicates that the anchor bolts and the surrounding plate retained most of their elastic responses.

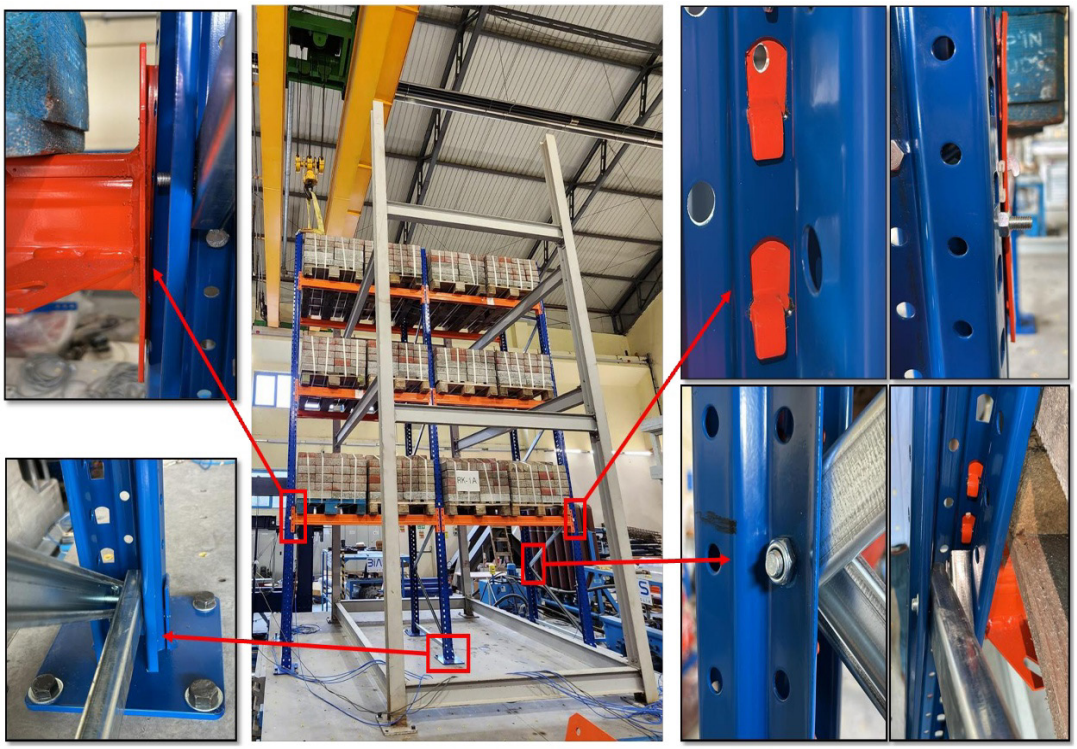

Figure 9 Experimental test results after 100% scale of the Northridge Earthquake.

The overall stability of the cold-formed elements was ensured in terms of buckling. Along their height, as their webs and flanges are still relatively straight, the uprights do not exhibit very high-frequency flexural or torsional-flexural buckling, except for local plate buckling near the holes and connection regions. Inconsiderable deformations at the diagonal bracing near the base (Figure 9) were observed owing to both inelastic bending and general buckling at the ends along the braces. This indicates that the rack system had not reached the load and buckling capacity, as these deformations were small and concentrated in small areas.

The experimental results revealed that the measured peak displacement values were significantly and substantially associated with the excitation scale, indicating a decrease in the effective stiffness of the rack system and suggesting local yielding or slipping between its members. Up to 50% of the scale of the Northridge earthquake, the rack system exhibited elastic behavior and had the ability to reverse its behavior. At larger-scale intensities, the rack system demonstrated more pronounced displacement amplification due to the free movement and sliding of the loading pallets on the beam. The absence of a mechanical constraint between the pallet and beam resulted in a weak response and significant amplification, resulting in more permanent and maximum displacement values, particularly at the third level.

At 10% of the Northridge seismic excitation, the pallets behaved as a sufficiently rigid frame with many degrees of freedom and self-centering capability on the rack structure because they moved without sliding on the beams, resulting in small maximum displacements of approximately 11.5, 15.9, and 28.9 mm on the first, second, and third floors, respectively. During this excitation, the displacement values were almost entirely concentrated around the origin (Figure 10), with small positive values for permanent displacements observed between approximately 3 and 11 mm, indicating that the displacement can be recovered over a very long period and that the structure was largely elastic. The permanent displacement was 11 mm relative to a peak displacement of 29 mm, which is an equivalent ratio of approximately 35-40%, which is the expected damping range when more damping than fracture is achieved, with only a slight connection slip, base oscillation, and asymmetric hysteresis loop at this seismic intensity.

At excitation levels of 20% to 40%, the rack system experienced almost linear peak displacements of values approximately 25-44 mm and 60-80 mm at the first and third levels, respectively (Figure 10). Under these excitations, the permanent displacements remained relatively small, with negative values at some levels. These small permanent displacements demonstrated that the rack system did not experience significant inelastic deformation, and the ability of the rack to re-center was destroyed by the full phase applied to the base of the rack at the end of the shaking, rather than by prior plasticity, which was also proved by the narrow hysteresis loops. Consequently, the permanent-to-peak displacement ratios were small, approximately less than 20-30%, indicating that pallet slipping was not developed, and the loss of stiffness and strength of the rack system was limited under these excitations.

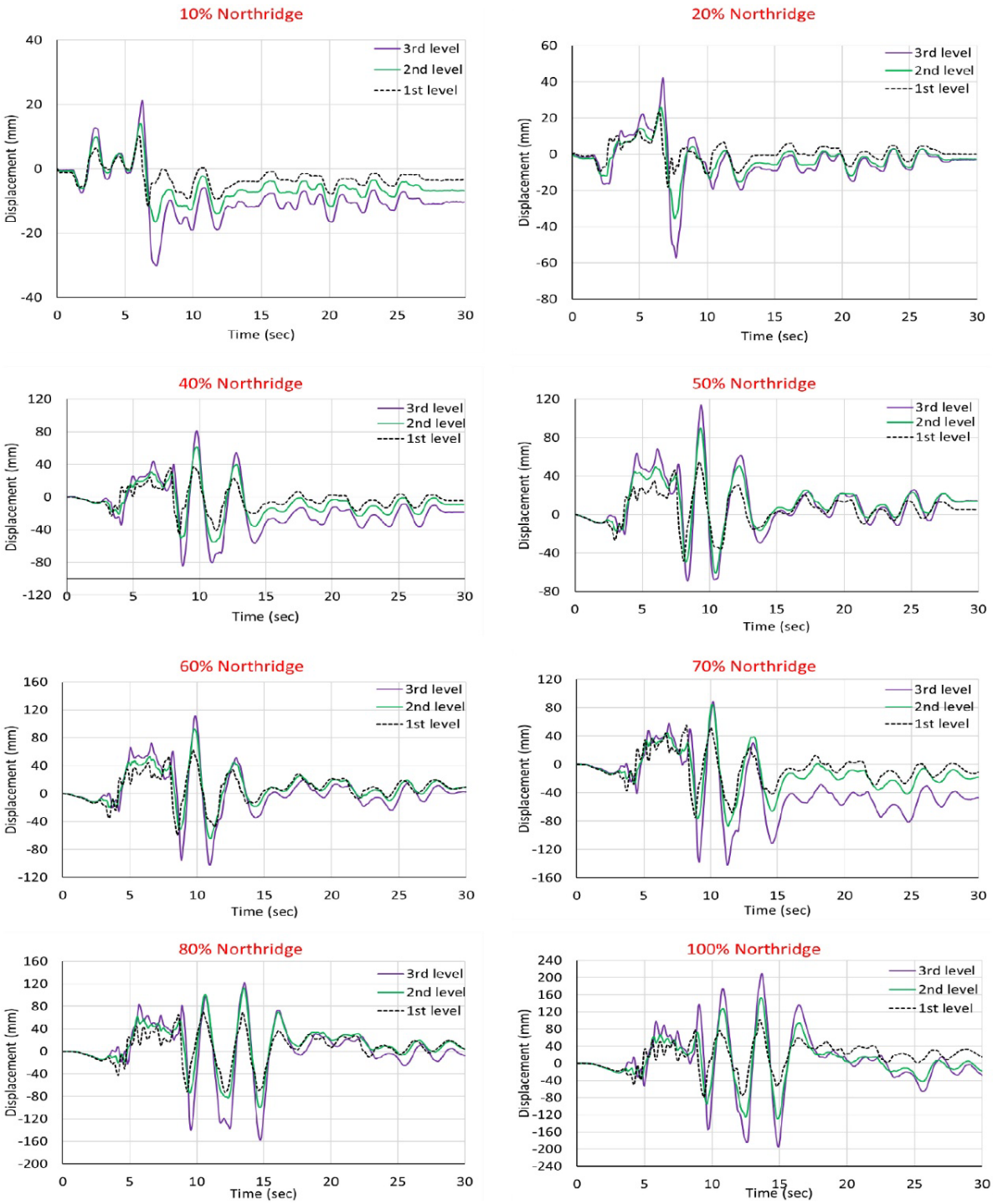

Figure 10 Response displacement results obtained from the experimental tests.

The results demonstrated that the system behavior changed qualitatively when the excitation reached 50% of the Northridge earthquake. At this excitation intensity, the maximum displacements observed at the top level were greater than 80-110 mm, associated with high negative values of the permanent displacements at all levels of -5.2 mm, -14.0 mm, and -14.1 mm. Because the magnitude of the permanent displacements has the same sign at all levels, it indicates that the rack is sliding in a single direction owing to the increasing cumulative inelastic deformations of the uprights and frictional sliding at the beam-upright connectors. Consequently, the pallet acquired a mobilization sense and began to slide relative to the beams, leading to the absorption of some of the seismic energy through sliding and impact, consequently widening their hysteretic loops and accumulating their self-centering ability. This implied a significant increase in the ratio of the permanent to peak displacement values and a more systematic structure, indicating a new response regime driven by the rack-pallet interaction and inelastic behavior.

At 60% and 70% of the Northridge earthquake, the maximum displacements increased, with peaks of 64–75 mm at the first level and 92–135 mm at the second and third levels, with negative medium values of the permanent displacements at the third level (approximately -2.4 to -9.4 mm and 11–47 mm at 60% and 70% of excitation, respectively). At 60% excitation, the third level has a peak of 111 mm with a permanent displacement of approximately -9 mm, whereas at 70% excitation, the third level has a peak of approximately 135 mm and a positive permanent displacement of approximately 47 mm (Table 3). During these excitation levels, the permanent displacement values were no longer proportional to the peak displacement, signifying that one pallet could be re-centered when the sliding changed direction, while other pallets and beams were left unbalanced owing to friction and impact damage, resulting in permanent rack drift. The change in the signal and applicability of the remnants leads to competition between these mechanisms.

During 80% to 100% of the Northridge seismic excitation, the maximum lateral displacements significantly increased, achieving values of approximately 70-102 mm at the lowest level of the structure and approximately 141-207 mm at the top levels (Figure 10). The permanent displacements were recorded as -4.1 mm, -4.1 mm, and 6.9 mm at 80% of the excitation and approximately -14.8 mm, 18.3 mm, and 28.1 mm at 100% of the excitation at the first, second, and third levels of the rack, respectively (Table 3). At 100% excitation intensity, the permanent-to-peak ratios at the top level of the rack were approximately 13–14%. However, the maximum residual values were large and positive, indicating that the rack experienced a strong, uniform lateral displacement and entered a highly inelastic response regime, with plastic deformations of the uprights, yielding or sliding of connections, and a repeated cycle of pallet sliding and impact, leading to irreversible displacements. This implies that the rack system loses its rigidity and may cause instability if subjected to subsequent vibrations, necessitating the inspection, realignment, and replacement of any affected structural elements.

The shaking table results demonstrated that changing the permanent displacement as the excitation intensity levels increased revealed a transition in behavioral modes, from primarily elastic behavior with small permanent displacement at lower excitation levels to substantial inelastic behavior with significant permanent displacements owing to connection slip and pallet sliding on the beam. This development in the permanent displacement with intensity at the observed levels is a powerful indicator that the stiffness deteriorated during the tests, as the structure had significant residual displacements following the main pulses. By comparing the ratio of the permanent to peak displacement results, especially around and after the 50% scale of excitation, it was found that the rack pallet system experiences a complex response: a pure elastic phase followed by a mixed elastic-plastic phase and subsequently a fully inelastic phase with substantial permanent displacements and cumulative damage in the system.

Table 3 Permanent displacement values observed from the experimental test results

	10%	20%	40%	50%	60%	70%	80%	100%
1st level	3.385	-0.041	4.344	-5.231	-2.398	11.137	-4.120	-14.835
2nd level	6.808	2.927	9.071	-13.950	-8.769	18.046	-4.121	18.305
3rd level	10.957	4.726	18.538	-14.118	-9.386	47.001	6.929	28.070

4 FINITE ELEMENT MODELING

A finite element mathematical model for the considered rack system was developed using ANSYS Workbench software (Engineering Simulation & 3D Design Software|Ansys, 2025R1) to capture the technical aspects of the complex behavior of rack systems under seismic loading. The finite element analysis used in this study involved shell and solid elements, with special consideration to the critical behavior of large deformations and post-buckling behavior (Figure 11). The structural elements (diagonal braces, beams, uprights, upright frames, and connection elements) were modeled using SHELL181 elements owing to the thin-walled nature of the structural elements used. SHELL181 was chosen because it can accurately model the behavior of rack components during seismic loading. It is a four-node element that is used appropriately for thin-mid-thick shell structures, and each node has six degrees of freedom (three translational and three rotational). This model allows for the representation of membrane bending and shear with sufficient accuracy, including nonlinearity.

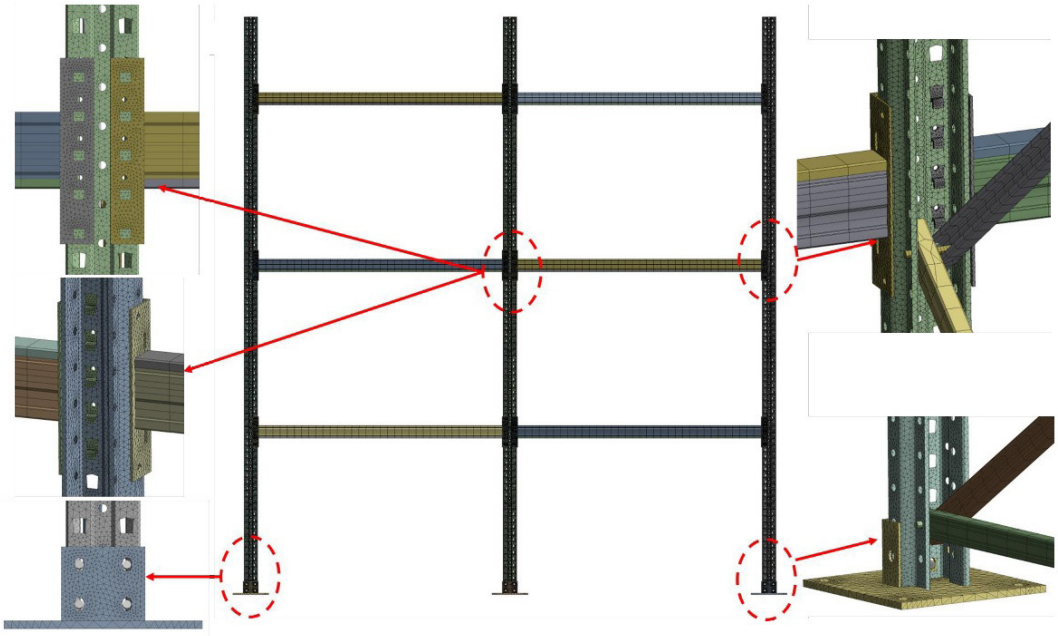

Figure 11 The FE mesh of the mathematical model.

The pinned joints between the uprights and diagonal or horizontal braces were SOLID187 elements (Figure 11) to model the complicated interaction between them. SOLID187 is a tetrahedral 10-node 3D-type element that can consider large deformations, material plasticity, and strain hardening. Because these models are large-scale and computationally complex, an explicit model of single bolts in the finite element analysis of the entire assembly is not feasible. In this regard, the idealization of bolt behavior was performed using BEAM188 elements in the numerical models, as shown in Figure 11. The BEAM188 element was used because it can model linear elastic behavior at large rotations and nonlinear material behavior at large strains. This method is useful for capturing the mechanical contribution of bolts and does not require a detailed geometry representation.

4.1. Loading and Boundary Conditions.

A two-step simulation process was executed in the ANSYS Workbench to execute the loading conditions placed on the rack systems. In the initial step, the pallet loads were assumed by assigning 1040 kg point masses to the beams, as shown in Figure 12. Two-point masses were concentrated on the surfaces of each beam. It is important to note that the finite element analysis also assumed that the point masses were completely stationary, thus ignoring the possibility of relative motion of the pallets along the beam. In the first step, the rack system was loaded in the vertical direction with an equivalent force of 12.48 kN, which was comparable to the gravitational effect. The second step involved the application of earthquake displacement time histories, which were applied to the support system in the experimental test, as shown in Figure 11. This lateral loading was implemented using nonlinear transient analysis by exciting the system in the down-aisle direction. To further assess the actual structural response, including stiffness, ductility, and seismic performance, the rack models were exposed to the actual Northridge earthquake records used in the experimental shaking table test (Figure 7), which allowed for an assessment of the post-yield behavior and failure modes.

The structural members forming the upright frames in a pallet stack system, such as vertical, horizontal, and diagonal bracing members, are typically connected via pinned joints. To accurately model this behavior in mathematical models, these connections were represented by edge-to-face bonded relationships constrained to a pin, thereby allowing for a realistic simulation of joint flexibility. The beam ends were welded to the connectors. In the finite element models, the end of the beam with its connector was therefore modeled as a bonded edge-to-face contact to reflect the rigid-welded condition. Four fasteners were used to connect the uprights to the baseplates on the backside. To represent these bolted connections in the FE model, the edge-face contact was defined as a no-separation contact, which is not only a fairly accurate model of the physical constraint but also permits sliding when a load is applied. To capture this in the FE model, the edges of the bolt holes on the base plate were fixed using the same boundary conditions (Ux = Uy = U z = 0). Conversely, the base plate in contact with the ground at its lower surface was constrained only in the vertical direction (Uz = 0), thereby allowing in-plane movement (Figure 12).

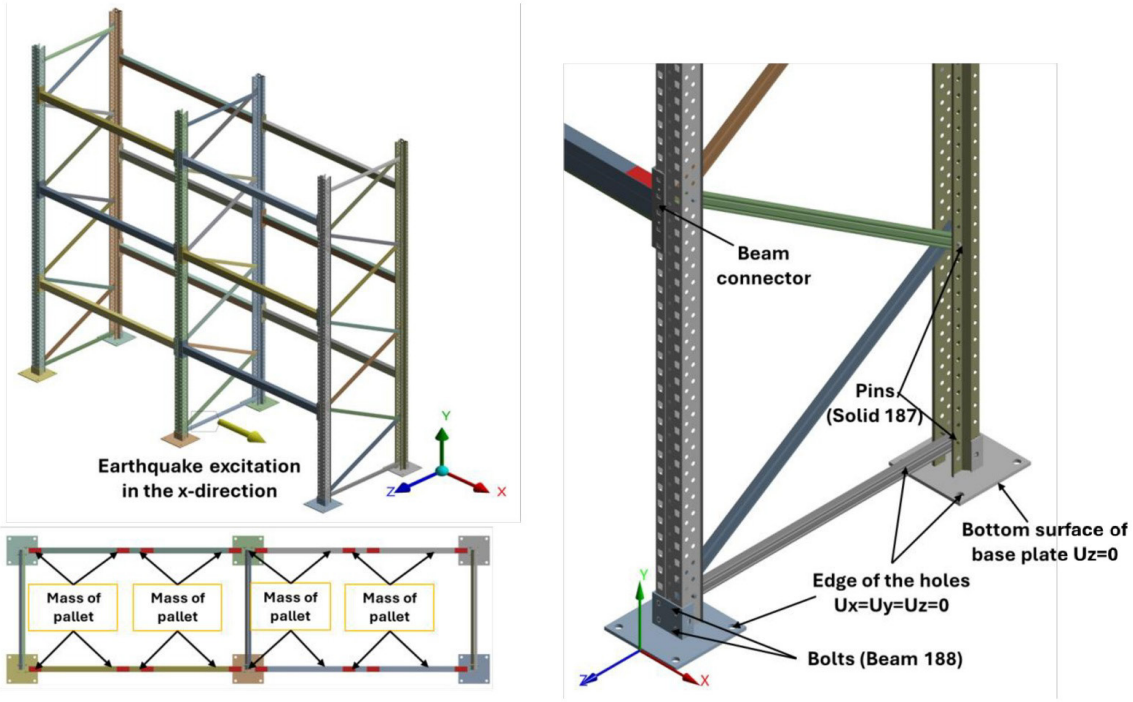

Figure 12 Boundary conditions and loading of the FE model.

5 RESULTS AND DISCUSSIONS

By analyzing and comparing the experimental and FE analysis results, it was clear that there was a great similarity in the response displacement time histories, accompanied by systematic trends whose properties depended on the excitation intensity and floor height. The finite element model results captured the main key features of the experimental response, such as the permanent periods and initial pulse, which appeared at approximately 10-12 seconds, and then the vibration began to decay after 20 s of the earthquake time, across all the scales of the Northridge excitations. Regarding the dominant pulse, peak displacement values, and overall response, the experimental results matched the results of the FE analysis at low to medium excitation levels because the pallets behaved as attached masses during the shaking test, often slightly greater at upper stories, presumably owing to the absence of further damping of behavior related to small connection slips and observed local buckling.

The finite element model and shaking table test revealed highly similar deformation patterns at both the global and local levels. Most of the localized deformations were concentrated at the beam-end connectors, connector tabs, and baseplate regions (Figure 13). Based on the finite element analysis, Von Mises stress was developed extremely high at the beam-upright connections, around the perforations in the uprights, and in the base plate regions, which then proves the validity of the critical regions in the rack systems subjected to seismic loads. Both results involved sway in the down-aisle direction associated with local and distortional buckling and slight tearing exhibited at the beam connectors and upright webs around the perforation holes and concentrated bearings around the anchor bolts (Figures 9 and 13).

The finite element results showed that the maximum stresses at 100% Northridge seismic excitation were near the nominal yield strength at the contact surfaces between the column, connector tabs, and bolt holes (Figure 13), indicating that localized yielding and plastic hinge mechanisms occurred in these areas. During the experimental full-scale test, local buckling and high permanent deformations were observed in the uprights and connector regions, demonstrating that the rack system had entered a highly inelastic state and that the geometric stiffness and stability had both significantly reduced, which confirms the key results predicted by the finite element models. The local out-of-plane buckling of the perforated uprights and deformation of the beam-connector interfaces (Figure 13), as in the test results (Figure 9), were similar to the high levels of stress and plastic strain concentration of the finite element results, and hence explain the strong residual drifts that occurred following the strong shaking. The local buckling modes were well predicted numerically by the finite element model, but the experimental buckling was much more irregular and asymmetric owing to manufacturing tolerances, initial imperfections, and the asymmetry of the loads imposed by pallet sliding, all of which caused somewhat higher residual deformations in the rack system and may have resulted in an earlier loss of load-carrying capacity than the idealized model. Based on the results, it can be said that the use of the numerical model of the rack system was more valid in determining the initiation and concentration of damage, even though the global displacements were underestimated because of neglecting the interaction behavior caused by the friction between the pallet and beams at a large scale of excitations.

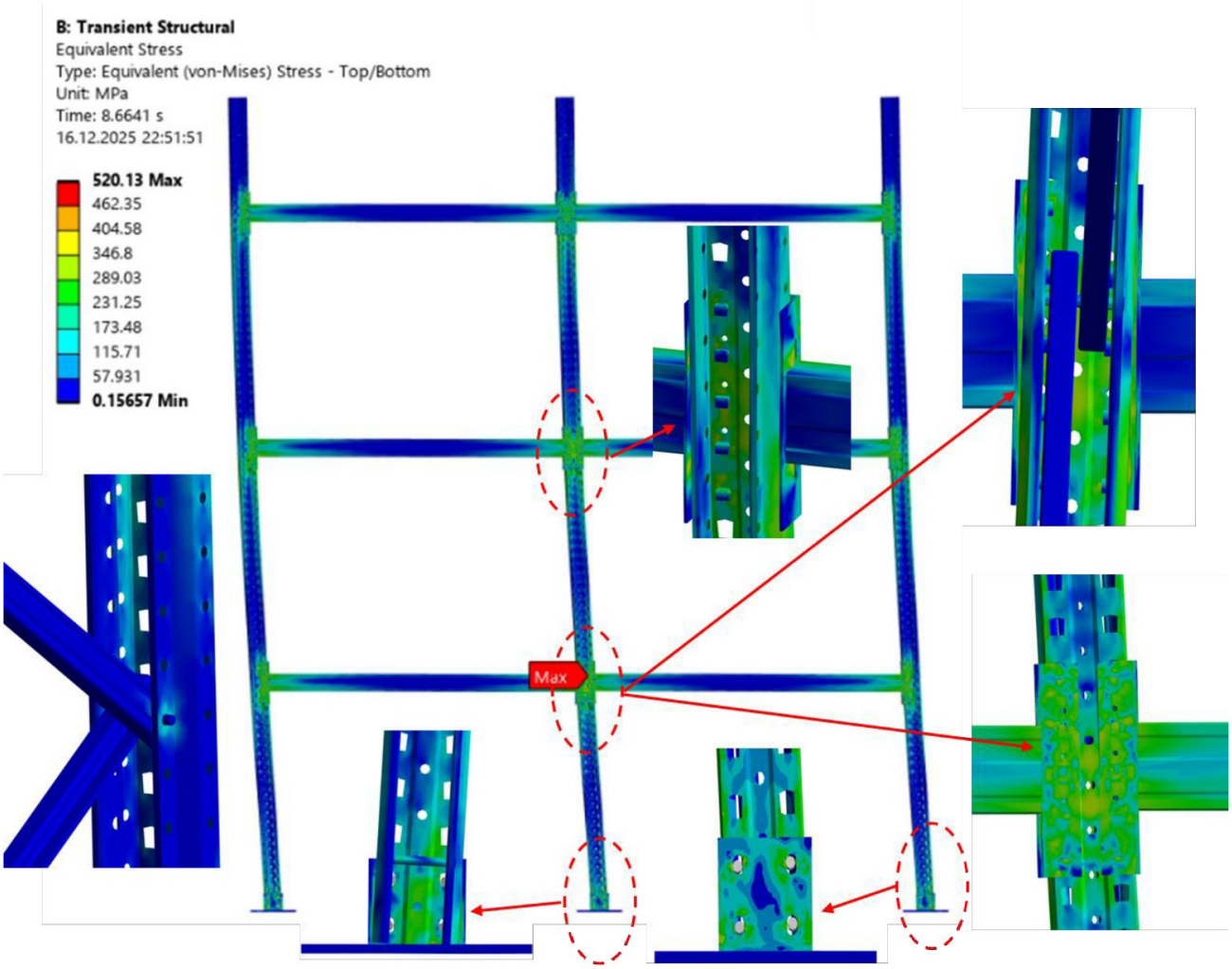

Figure 13 Von miss stress distribution of the rack system under 100% of the Northridge records

The experimental peak displacements in the upper levels increased significantly with systematic deviations in the results compared to the FE predictions after exceeding 60% of the excitation level (Figures 14 and 15). This difference in the results is because, during the experimental test, the wooden pallet began to slide, and the friction between the connections and the other members of the rack systems began to activate at higher excitation levels. Although frame deformations are still a controlling factor in the FE model, indicating that the rack response is well replicated by the numerical models, the response displacement of the rack systems is affected by the unrestrained interactions between the loading pallets and beams, especially at higher excitation intensities.

At the lowest level, the finite element (FE) and experimental results agreed in phase almost perfectly (Figure 14), but still showed significant differences in amplitude, indicating that the parameters of stiffness and assigned mass were sufficiently replicated in the FE modeling, but boundary conditions and base-plate flexibility may nonetheless cause an underestimation of damping in the FE model. At the second and third levels, the experimentally measured displacements had a slightly enhanced content of high frequencies with a stronger permanent displacement after the main pulse, indicating locally occurring nonlinearities and slipping at connections that were either smoothed or idealized in the entire-tie connection modelling simulated in the FE modelling.

Based on the maximum values of the displacement time history results, the finite element model (FE) reproduced the experimentally determined maximum displacements with high validity, with similarity ratios exceeding 0.80 and even higher (Table 4). At the excitation level considered, the average similarity ratio was approximately 0.83, indicating that the variations between the FE and experimental peak displacements were usually less than 20%. Such a level of agreement is generally acceptable for validating the nonlinear dynamic FE models of rack-type structures under seismic loading, particularly when variability in material properties, connection behavior, and measurement noise is considered.

Table 4 Comparison of experimental and FE maximum response displacement results.

Story	Result	Northridge excitation scale							
		10%	20%	40%	50%	60%	70%	80%	100%
1st Level	Exp. Peak	11.52	25.12	44.03	64.08	-64.17	75.15	70.79	-101.85
	FE. Peak	16.1	33.35	52.81	54.39	76.67	76.98	80.69	-101.7
	Similarity ratio	0.72	0.75	0.83	0.85	0.84	0.98	0.88	0.98
2nd Level	Exp. Peak	19.36	41.66	61.27	89.82	-92.67	-84.79	97.39	-152.59
	FE. Peak	15.93	34.56	60.96	74.3	90.72	83.9	90.13	-109.09
	Similarity ratio	0.82	0.83	0.99	0.83	0.98	0.99	0.93	0.71
3rd Level	Exp. Peak	21.98	49.05	80.9	111.59	-111.11	134.81	141.24	-207.04
	FE. Peak	28.93	57.17	70.84	82.21	99.19	90.67	-104.63	-120.23
	Similarity ratio	0.76	0.86	0.88	0.74	0.89	0.67	0.74	0.58

At 100% scale of Northridge excitation, frictional behavior and impact mechanisms were activated because of the pallet sliding on the beams and connection slip during the test, leading to more complex asymmetric hysteresis loops (Figure 16), resulting in effectively dissipating energy and changing the center of mass, sudden decreases, and significant loss of secant and tangent stiffness of the rack as the pallets were re-centered. Frictional damping caused the interaction effects to reduce the force exerted on the rack at every level and then increase the permanent displacements. In addition, the base shear forces did not increase proportionately, which explains why greater peak displacements were exhibited in the experiments than those in the finite element analysis at large-scale excitations. Consequently, it can be said that a clear inclusion of loading pallet-beam contact and possible loss of connection properties may be required to fully replicate the observed energy-dissipation capacity estimations and loss of stiffness of the tested rack-pallet systems.

The hysteresis and backbone curves (Figure 16) provided a clear succession of the relation between the base shear forces and top peak displacements, as the curves started with relatively narrow and stable loops at 10-20% of Northridge excitation and then gradually increased in pinching and weakened over time as the excitation changed to 60-100%. The finite element analysis results showed that at every scaling level, the backbone envelopes were approximately linear in nature at first, and that they were followed subsequently by a more and more pronounced weakening and softening, similar to yielding and local buckling phenomena found in uprights and beam-column connections. Compared with the experimental results measured on pallet racks, the simulation loops were smoother, with fewer sudden drops in stiffness. This difference shows that the finite element model effectively predicted the nonlinearity of the materials and geometrical effects, but it could not include all contributors of friction and impact, pallet beam slip, and connection discontinuities.

The peak base shear and the related displacement along the backbone curves were calculated, as shown in Figure 16. The corresponding transitional (secant) stiffnesses were calculated by dividing the maximum shear force by the maximum response displacement at the top of the rack (Table 5). The equivalent transitional stiffness of the system was observed to be approximately 0.40, 0.38, 0.29, 0.27, 0.25, 0.23, 0.20, and 0.20 kN/mm increments at excitation levels of 10 to 100%, thus revealing a total of approximately 50% decrease in the effective lateral stiffness. The results showed that the system was relatively rigid at low-intensity motions (10-20% scale), indicated by the steep slope and almost linear envelopes through the range of displacement, with a secant stiffness near 0.4 kN/mm. Beyond a 40% scale of excitation, the curve of the backbone flattened, and the effect of further displacement on the increase in the base shear was further minimized. This effect is explicitly reflected in the decrease in transitional stiffness to 0.2 kN/mm at 80–100% scale of the excitation, thus denoting a significant yielding and softening of the global lateral system.

Regarding peak shear forces, the increase in base shear peaks by the order of 6 kN at small drifts (approximately 15 mm) to approximately 30 kN at large drifts (approximately 150 mm), but the rate of increase is clearly sublinear; the addition of displacement beyond a value of 70-80 mm produces only a relatively small increase in shear resistance. This effect is supported by the decreasing values of transitional stiffness and indicates that the rack goes through a highly inelastic regime under the influence of high intensities, where the rack undergoes a large amount of residual deformation with a minor increase in the resisting force, raising concerns about serviceability, connection rupture, and the safety of stored goods under strong seismic activities.

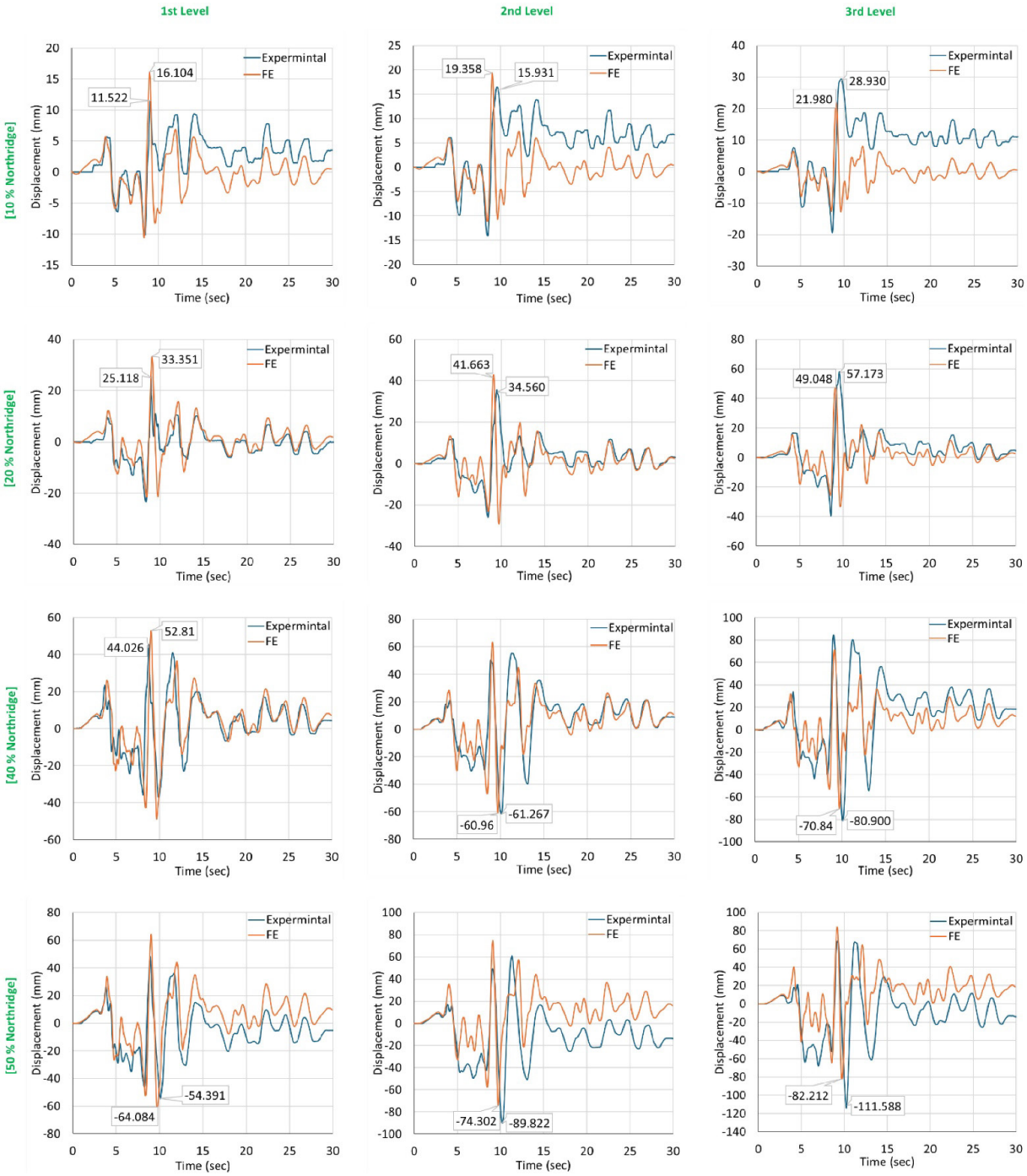

Figure 14 Comparison of response displacement between FE and experiments under a 10-50% scale of the Northridge excitation.

Table 5 FE results of the transitional stiffness and energy dissipation capacity for the rack system

Northridge scale	Max. Shear Force (KN)	Max. Displacement (mm)	Transitional stiffness (KN/m)	Energy dissipation KN.m
10%	6	15	0.4	0.145
20%	15	40	0.38	0.799
40%	20	70	0.29	2.233
50%	23	85	0.27	3.332
60%	25	100	0.25	3.597
70%	27	115	0.23	5.012
80%	28	140	0.20	5.679
100%	30	150	0.20	7.174

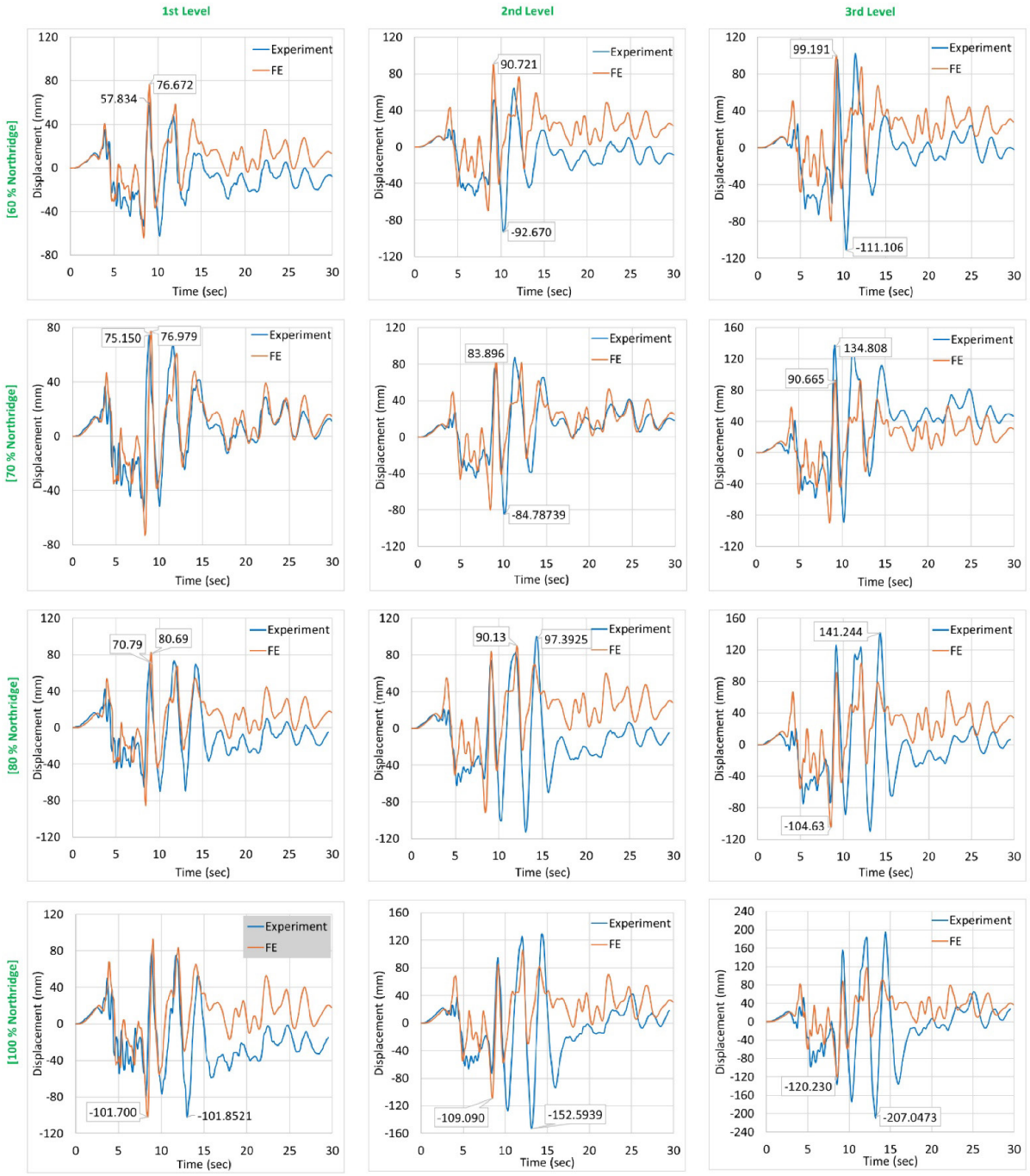

Figure 15 Comparison of response displacement between the FE and experimental under a 60-100% scale of the Northridge excitation.

The energy dissipation ability (Table 5) showed a steep increase as the magnitude of excitation increased, as shown in the cumulative measures of dissipation energy: 0.145 KN.m at 10% NE, 0.799 KN.m at 20% NE, 2.233 KN.m at 40% NE, 3.332 KN.m at 50% NE, 3.597 KN.m at 60% NE, 5.679 KN.m at 70% NE, and 7.174 KN.m at 100% NE (Table 5). The combination of this increase in cumulative energy with an associated increase in the size of the hysteresis loop area showed that the rack system increasingly becomes dependent on hysteretic and frictional processes to dampen the seismic input. Nonetheless, at high excitation levels, the subsequent degradation of the rack structure, in terms of greater damage and degradation of structural integrity, indicated that this form of energy dissipation was achieved at the expense of major structural damage. This degradation was more clearly observed in the change in the shape of the hysteresis loop with scale: the loops became narrower, the unloading and reloading grew closer to the origin, and one step-scale-level cycle was found to have a lower load than the previously observed cycles. This behavior, coupled with the steady reduction in the secant stiffness, represents a cyclic loss of stiffness and strength, which is presumably controlled by the inelastic behavior and slipping at the beam-to-column and base connections of pallet rack systems.

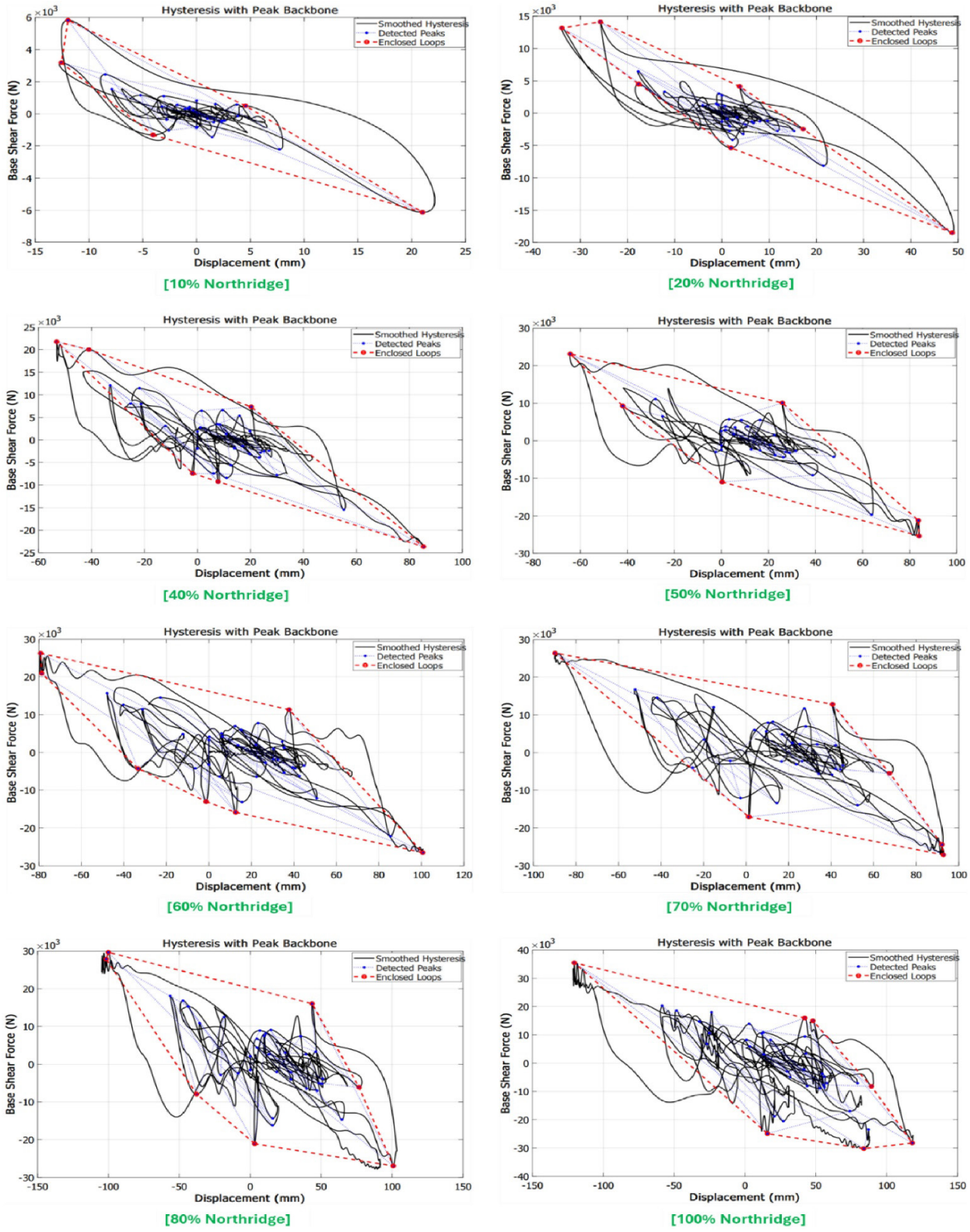

Figure 16 Base shear vs. displacement hysteresis curve of the rack system obtained from FE analysis.

6 CONCLUSIONS

This study investigates the down-aisle seismic response of a conventional cold-formed steel storage rack subjected to scaled Northridge earthquake records, by means of full-scale experimental testing and a calibrated finite element model. Particular attention is devoted to elucidating the influence of inelastic connection behavior and pallet–rack interaction on the system's dynamic response, damage progression, and energy dissipation capacity.

- The rack withstood 100% Northridge excitation without global collapse but developed notable residual drifts and localized damage at beam–upright, brace–upright, and base-plate connections.
- The response remained essentially elastic up to about 40–50% of the Northridge scale; above this, strong inelastic behavior, stiffness loss, and permanent drift developed, especially at upper levels.
- The FE model, calibrated in mass, stiffness, and boundary conditions, reproduced the main dynamic features and peak displacements with similarity ratios often above 0.80 up to about 50% excitation.
- For excitation levels of 60% and higher, unconstrained pallet sliding and rocking substantially amplified and irregularized the response displacements, introducing additional frictional and impact-based energy-dissipation mechanisms that were not captured in the simplified finite element model.
- At 60–100% excitation, the FE model underestimated peak and residual displacements because it did not explicitly include pallet sliding and impact, connection slip, friction, and geometric imperfections.
- The dissipated energy rose from 0.145 kN·m at 10% to 7.174 kN·m at 100%, showing increasing reliance on hysteretic and frictional mechanisms accompanied by severe damage and stiffness degradation at high intensities.
- The effective lateral stiffness dropped by about 50%, from roughly 0.4 kN/mm at 10% excitation to about 0.2 kN/mm at 100%, consistent with larger displacements and residual deformations.
- Both tests and simulations identified critical stress regions at beam–upright connections, upright perforations, and base plates, matching observed local buckling, distortion, and damage.
- Despite nonlinear materials, the FE model produced smoother hysteresis and milder stiffness degradation than the experiments, which showed more pinched loops, abrupt stiffness drops, and asymmetric buckling due to slip, friction, and initial imperfections.
- The results show that although cold-formed steel rack systems can avoid collapse under strong earthquakes, their seismic performance is governed by connection nonlinearity, pallet to beam interaction, and stiffness degradation, underscoring the need to model these mechanisms explicitly and to refine seismic design provisions for storage racks.

Author's Contributions: Conceptualization, Fuat Yılmaz and Fatih Alemdar; Methodology, Fuat Yılmaz and Fatih Alemdar; Investigation, Fuat Yılmaz; Writing - original draft, Fuat Yılmaz; Writing - review & editing, Fatih Alemdar; Funding acquisition, Fuat Yılmaz and Fatih Alemdar; Resources, Fuat Yılmaz and Fatih Alemdar; Supervision, Fatih Alemdar

Data Availability statement: No research data were used

Editor: Marco L. Bittencourt

References

Aguirre, C. (2005). Seismic behavior of rack structures. Journal of Constructional Steel Research, 61(5), 607–624. https://doi.org/10.1016/j.jcsr.2004.10.001.

Bernuzzi, C., & Simoncelli, M. (2017). Steel storage pallet racks in seismic zones: Advanced vs. standard design strategies. Thin-Walled Structures, 116, 291–306. https://doi.org/10.1016/j.tws.2017.03.002.

Bonaventura, T., Montuori, R., Vayas, I., Antonodimitraki, S., Titirla, M. D., Simoncelli, M., & Lignos, X. (2021). Experimental testing campaign and numerical modelling of an innovative base-plate connection for pallet racking systems. COMPDYN Proceedings, 2934–2942. https://doi.org/10.7712/120121.8687.19514.

Bové, O., Ferrer, M., Almansa, F. L., & Roure, F. (2021). Comparison Between Two Types of Seismic Tests of Racking Systems. Ce/Papers, 4(2-4), 1992–1998. https://doi.org/10.1002/cepa.1513.

C.A. Castiglioni, N. Panzeri, J. Brescianini, P. Carydis, Shaking table tests of steel pallet racks, in: Proceedings of the Conference on Behaviour of Steel Structures in Seismic Areas-Stessa 2003, Naples, Italy, 2003, pp. 775–781.

Carlo Andrea Castiglioni. (2016). Seismic behavior of steel storage pallet racking systems, Cham Springer International Publishing.

Çelik,İ., Yildiz, İ.D., Arslan, K. Y., Yusuf Öztürk, Mehmet Erkan Efe, & Tevfik Burak Kocaman. (2022). Effect of base-plate types on system behaviour in down-aisle pallet rack systems. Journal of Constructional Steel Research, 198, 107584. https://doi.org/10.1016/j.jcsr.2022.107584.

Chen, C., Shi, L., Mahdi Shariati, Toghroli, A., Mohamad, E. T., Bui, D. T., & Majid Khorami. (2019). Behavior of steel storage pallet racking connection - A review. Steel and Composite Structures, 30(5), 457–469. https://doi.org/10.12989/scs.2019.30.5.457.

Drei, A., Rovere, L., Vayas, I., Jehin, D., Orsatti, B., Kanyilmaz, A., Braham, C., Hoffmeister, B., Cudini, T., Sesana, S., Bakalbasis, D., Konstantinos, A., Bernuzzi, C., Kraus, O., Hermanek, J., Degee, H., Castiglioni, C. A., Frederiks, J. W., & Heinemeyer, C., (2014). Seismic behaviour of steel storage pallet racking systems (SEISRACKS2) : final report, Publications Office of the European Union, (Luxembourg). https://data.europa.eu/doi/10.2777/686466.

Engineering Simulation & 3D Design Software | Ansys. (2025). Www.ansys.com. http://www.ansys.com.

Filiatrault, A. and, Wanitkorkul, A. (2004). Shake-Table Testing of Frazier Industrial Storage Racks, Report No. CSEE-SEESL-2005-02, Structural Engineering and Earthquake Simulation Laboratory, Department of Civil, Structural and Environmental Engineering, University at Buffalo, State University of New York.

Firouzianhaji, A., Usefi, N., Samali, B., & Mehrabi, P. (2021). Shake Table Testing of Standard Cold-Formed Steel Storage Rack. Applied Sciences, 11(4), 1821. https://doi.org/10.3390/app11041821.

Gilbert, B. P., & Rasmussen, K. J. R. (2010). Bolted moment connections in drive-in and drive-through steel storage racks. Journal of Constructional Steel Research, 66(6), 755–766. https://doi.org/10.1016/j.jcsr.2010.01.013.

Gilbert, B. P., & Rasmussen, K. J. R. (2011). Determination of the base plate stiffness and strength of steel storage racks. Journal of Constructional Steel Research, 67(6), 1031–1041. https://doi.org/10.1016/j.jcsr.2011.01.006.

Heo, G., Ko, B., Seo, Y., & Kim, C. (2023). Analysis of behavioral characteristics according to the fixing condition of pallet rack. Journal of Constructional Steel Research, 203, 107844. https://doi.org/10.1016/j.jcsr.2023.107844.

Jacobsen, E. and Tremblay, R. (2017). Shake-table testing and numerical modelling of inelastic seismic response of semi-rigid cold-formed rack moment frames. Thin-Walled Structures, 119, pp.190–210. https://doi.org/10.1016/j.tws.2017.05.024.

Kanyilmaz, A., Brambilla, G., Chiarelli, G. P., & Castiglioni, C. A. (2016). Assessment of the seismic behaviour of braced steel storage racking systems by means of full-scale push-over tests. Thin-Walled Structures, 107, 138–155. https://doi.org/10.1016/j.tws.2016.06.004.

Maguire, J. R., Teh, L. H., Clifton, G. C., Tang, Z. H., & Lim, J. B. P. (2020). Cross-aisle seismic performance of selective storage racks. Journal of Constructional Steel Research, 168, 105999. https://doi.org/10.1016/j.jcsr.2020.105999.

Nuñez, E., Aguayo, C., & Herrera, R. (2020). Assessment of the Seismic Behavior of Selective Storage Racks Subjected to Chilean Earthquakes. Metals, 10(7), 855. https://doi.org/10.3390/met10070855.

Petrone, F., Higgins, P. S., Bissonnette, N. P., & Kanvinde, A. M. (2016). The cross-aisle seismic performance of storage rack base connections. Journal of Constructional Steel Research, 122, 520–531. https://doi.org/10.1016/j.jcsr.2016.04.014.

Petrovčič, S., & Kilar, V. (2012). Effects of Horizontal and Vertical Mass-Asymmetric Distributions on the Seismic Response of a High-Rack Steel Structure. Advances in Structural Engineering, 15(11), 1977–1988. https://doi.org/10.1260/1369-4332.15.11.1977.

Prabha, P., Marimuthu, V., Saravanan, M., & Arul Jayachandran, S. (2010). Evaluation of connection flexibility in cold-formed steel racks. Journal of Constructional Steel Research, 66(7), 863–872. https://doi.org/10.1016/j.jcsr.2010.01.019.

Saravanan, M., Marimuthu, V., Prabha, P., Surendran, M., & Palani, G. S. (2014). Seismic characterization of cold-formed steel pallet racks. Earthquakes and Structures, 7(6), 955–967. https://doi.org/10.12989/eas.2014.7.6.955.

Shaheen, M. S. A., & Rasmussen, K. J. R. (2019). Seismic tests of drive-in steel storage racks in cross-aisle direction. Journal of Constructional Steel Research, 162, 105701. https://doi.org/10.1016/j.jcsr.2019.105701.

Sideris, P., Filiatrault, A., Leclerc, M., & Tremblay, R. (2010). Experimental Investigation on the Seismic Behavior of Palletized Merchandise in Steel Storage Racks. Earthquake Spectra, 26(1), 209–233. https://doi.org/10.1193/1.3283389.

Vujanac, R., Miloradović, N., Vulović, S., & Pavlović, A. (2020). A Comprehensive Study into the Boltless Connections of Racking Systems. Metals, 10(2), 276. https://doi.org/10.3390/met10020276.